Biophysical Journal Volume 65 October 1993 1718–1726

# Time-resolved Absorption and Magnetic Circular Dichroism Spectroscopy of Cytochrome $c_3$ from *Desulfovibrio*

Donald B. O'Connor,*‡ Robert A. Goldbeck,* Jo H. Hazzard,§¶ David S. Kliger,* and Michael A. Cusanovich§

*Department of Chemistry and Biochemistry, University of California, Santa Cruz, California 95064, and §Department of Biochemistry, University of Arizona, Tucson, Arizona 85721 USA

ABSTRACT The UV-visible absorption and magnetic circular dichroism (MCD) spectra of the ferric, ferrous, CO-ligated forms and kinetic photolysis intermediates of the tetraheme electron-transfer protein cytochrome $c_3$ (Cc3) are reported. Consistent with bis-histidinyl axial coordination of the hemes in this Class III *c*-type cytochrome, the Soret and visible region MCD spectra of ferric and ferrous Cc3 are very similar to those of other bis-histidine axially coordinated hemeproteins such as cytochrome $b_5$. The MCD spectra indicate low spin state for both the ferric ($S = ½$) and ferrous ($S = 0$) oxidation states. CO replaces histidine as the axial sixth ligand at each heme site, forming a low-spin complex with an MCD spectrum similar to that of myoglobin-CO. Photodissociation of Cc3-CO (observed photolysis yield = 30%) produces a transient five-coordinate, high-spin ($S = 2$) species with an MCD spectrum similar to deoxymyoglobin. The recombination kinetics of CO with heme Fe are complex and appear to involve at least five first-order or pseudo first-order rate processes, corresponding to time constants of 5.7 μs, 62 μs, 425 μs, 2.9 ms, and a time constant greater than 1 s. The observed rate constants were insensitive to variation of the actinic photon flux, suggesting noncooperative heme-CO rebinding. The growing in of an MCD signal characteristic of bis-histidine axial ligation within tens of microseconds after photodissociation shows that, although heme-CO binding is thermodynamically favored at 1 atm CO, binding of histidine to the sixth axial site competes kinetically with CO rebinding.

## INTRODUCTION

The cytochromes $c_3$ (Cc3) are found in the sulfate-reducing bacteria of the genus *Desulfovibrio* (Ishimoto et al., 1954; Postgate, 1954), where they are believed to function as electron carriers for hydrogenase (Suh and Akagi, 1969; Tamura et al., 1988). The Cc3 have unique structural properties in comparison to most other *c*-type cytochromes in that they contain four hemes covalently bound to a single polypeptide of only 100–120 amino acids, similar in size to the monoheme cytochromes (13–15 kDa). The four heme groups have histidines as axial ligands in both the 5th and 6th coordination sites (Class III) in contrast to the eukaryotic Class I *c*-type cytochromes, such as mitochondrial cytochrome *c*, which have methionine in the 6th position and Class II *c*-type cytochromes, such as cytochrome *c'*, which do not have a 6th ligand. The heme groups of Cc3 have a much greater exposure to solvent (127–168 Å$^2$) than does the single heme group of the mitochondrial cytochromes *c* (32–49 Å$^2$) (Higuchi et al., 1984). As a result of these unique structural features, the Cc3 exhibit a number of unusual physiochemical properties. The reduction potentials of the four Cc3 heme groups are very low, resulting in macroscopic reduction potentials linking the five macroscopic oxidation states of Cc3 that range from −240 to −357 mV *vs.* NHE for Cc3 from *Desulfovibrio vulgaris* Miyazaki F (Niki et al., 1987). Solid films of reduced Cc3 exhibit a very high conductance (Kimura et al., 1979; Nakahara et al., 1980), a property which may provide useful applications for Cc3 in bioelectronics.

The fully reduced form of Cc3 binds ligands such as carbon monoxide (CO) at the sixth coordination position of each of the four hemes (Yagi and Maruyama, 1971). Unlike most other hemeproteins that bind CO to the ferrous heme iron (Fe) such as myoglobin, hemoglobin, cytochrome *c'*, cytochrome *c* oxidase, and cytochrome *c* peroxidase, the ferrous Cc3 hemes do not have a vacant sixth coordination position. Thus, all species of Cc3 that have been studied spectroscopically to date have predominantly low-spin character. It is reasonable to presume that the sixth position (distal) histidine must dissociate from the heme Fe before ligand binding can occur in Cc3, creating a transient, high-spin intermediate. As is typical for CO complexes of hemeproteins, the Fe-CO bond can be broken in Cc3 by laser flash photolysis, generating a transient ferrous heme Fe species to which free CO recombines in a second order rate process. Therefore, at least two circumstances exist in which a five-coordinate Cc3 heme Fe species may be generated, at least transiently.

The near-UV and visible optical spectroscopy of cytochromes provides information regarding the oxidation state and axial ligation of the heme iron (Moore and Pettigrew, 1990). The electronic absorption bands, commonly referred to as the Soret and Q bands, involve electronic $\pi$-$\pi^*$ transitions of the porphyrin chromophore. The Coulombic interaction of the heme iron with the $\pi$ orbital electrons of the porphyrin ring influences the electronic energy levels. Hence, electronic absorption spectra are sensitive to the charge, i.e., oxidation state, of the iron. Ligands influence the

*Received for publication 7 May 1993 and in final form 16 July 1993.*

Address reprint requests to R. A. Goldbeck, Department of Chemistry and Biochemistry, University of California, Santa Cruz, CA 95064. Tel.: 408-459-4007 (office); Fax: 408-459-2935; e-mail: goldbeck@chemistry.ucsc.edu.

‡Present address: Center for Fast Kinetics Research, University of Texas, Austin, TX 78705.

¶Present address: Department of Biochemistry and Molecular Biophysics, Washington University School of Medicine, 660 S. Euclid Ave., St. Louis, MO 63110.



0006-3495/93/10/1718/09 $2.00

electronic structure of the heme iron and thus can also influence the porphyrin transitions. In particular, electronic absorption bands can indicate both the number of and nature of the axial ligands. Additional electronic transitions in the visible involving charge transfer among the iron, ligand, and porphyrin ring orbitals are also possible, although these transitions are relatively weak.

Magnetic circular dichroism (MCD), the differential absorption of right and left circularly polarized light, offers information that is complementary to electronic absorption spectroscopy (Dawson and Dooley, 1989). MCD is particularly sensitive to the spin state of the heme iron. Thus, MCD is adept at distinguishing high-spin five-coordinate hemeproteins from low-spin six-coordinate hemeproteins. Until recently, MCD was not particularly useful in studying transient species because of the approximately millisecond time resolution of conventional CD spectrometers. The MCD spectra of shorter-lived metastable species could only be obtained by low-temperature trapping. The advance of time-resolved MCD (TRMCD) and time-resolved circular dichroism (TRCD) to the nanosecond time regime offers promise in characterizing short-lived structures of porphyrins, hemes, and cytochromes (Lewis and Kliger, 1987; Goldbeck et al., 1989; Goldbeck and Kliger, 1993) at physiologically relevant temperatures. The present study demonstrates the usefulness of TRMCD in characterizing the transients of CO-ligated Cc3 that are formed after laser photolysis.

We present here the MCD and absorption spectra of equilibrium and time-evolving forms of Cc3 from *Desulfovibrio vulgaris* strain Hildenborough. The spectra of the equilibrium ferric and ferrous forms of the protein and the complex with all hemes axially ligated in the sixth position to carbon monoxide (Cc3-CO) are presented. Most significantly, we examine the TRMCD and transient absorption (TROD) spectra of Cc3-CO on a time scale from nanoseconds to milliseconds after laser photolysis of the CO ligand. The spectral features and time evolution of these spectra add insight into the structural nature of the short-lived intermediates. In particular, we find that in addition to the second order recombination of CO with Cc3 there is a fast intraprotein coordination of histidine to the sixth, axial heme site.

## MATERIALS AND METHODS

Cc3 was purified from *D. vulgaris* Hildenborough strain by the method of Bartsch (Akutsu et al., 1992). All samples were prepared in pH 7.0, 0.1 M potassium phosphate buffer. Reduced cytochrome was prepared by saturating the buffer solution with either argon or nitrogen, then adding sodium dithionite and sample. The CO-ligated cytochrome was prepared similarly with CO substituted for the argon or nitrogen. After preparation of the sample, the gas-saturated sample solution was sealed. A peristaltic pump continuously flowed Cc3 solution through the sample cell during time-resolved MCD and absorption measurements, insuring that each optical pulse probed fresh sample. Due to the relative ease with which the cytochrome is oxidized and the oxygen permeability of the soft tubing used in the peristaltic pump, the head of the pump was enclosed and flushed continuously with N2 and the connection from the pump housing to the sample cell was made with stainless steel tubing. Reduced samples were typically stable in this configuration for 2–4 days.

Room temperature (20 ± 1°C) absorption spectra were recorded with a diode array spectrophotometer (Hewlett Packard model 8452A, single beam, 2-nm resolution). Subtraction of the absorbance of neat buffer solution from the absorbance of protein solution measured in the same cell yielded the absorption due solely to cytochrome. TROD and TRMCD spectra were measured at ambient temperature (22 ± 1°C) on an apparatus that is described elsewhere (Lewis and Kliger, 1987; Goldbeck et al., 1989; Goldbeck and Kliger, 1993).

## RESULTS AND DISCUSSION

### Ferric cytochrome $c_3$

Fig. 1 shows the ground state electronic absorption spectrum of ferric (oxidized) Cc3. The spectral characteristics, summarized in Table 1, agree with published data (Meyer and Kamen, 1982; Drucher et al., 1970). The prominent spectral bands are the intense Soret absorption ($\lambda_{max}$ ~410 nm) and the much weaker and very broad visible absorption ($\lambda_{max}$ ~530 nm). The general features of ferric Cc3 absorption are common to low-spin ($S$ = 1/2) ferric heme proteins with histidine-methionine axial ligation such as class I cytochromes *c* (Moore and Pettigrew, 1987) as well as with bis-histidine axial ligation such as cytochrome $b_5$ (see Table 1) (Dolinger et al., 1974; Ozols and Strittmatter, 1964). Ferric Cc3 does not exhibit a weak absorption band around 640 nm as do high-spin ferric heme proteins (Moore and Pettigrew, 1987).

The MCD spectrum of ferric Cc3 is shown in Fig. 2 and the extrema and zero crossings are detailed in Table 1. The symmetrical "S" shaped band in the Soret resembles the first derivative of the absorption and the zero crossing corresponds closely with the absorption maximum. The Soret MCD of other low-spin ferric heme proteins, particularly cytochrome $b_5$ (Dolinger et al., 1974; Vickery et al., 1975), have similar features (Table 1). Temperature dependence studies (Vickery et al., 1976a) have shown this band to be composed of $C$ terms arising from the coupling of the degenerate spin states of paramagnetic, low spin ($S$ = ½) iron III with the porphyrin $\pi$-$\pi^*$ transitions. Vickery et al. (1976b) have postulated that the intensity of the Soret MCD of ferric heme complexes is proportional to the extent of low

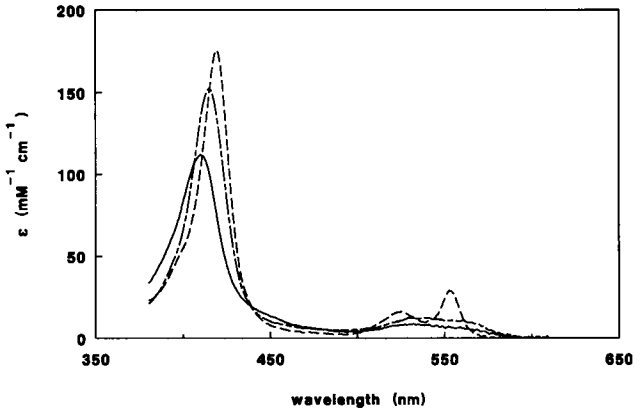


FIGURE 1 Soret and visible band absorption spectra of ferric (——), ferrous (- - - -), and ferrous-CO (— - —) forms of cytochrome $c_3$.

**TABLE 1 Spectral features of the electronic absorption and magnetic circular dichroism of ferric (oxidized), bis-histidine, heme proteins**

| Absorption | Soret band $\lambda_{max}$ | Soret band $\epsilon$ (cm mM)$^{-1}$ per heme | Visible band $\lambda_{max}$ | Visible band $\epsilon$ (cm mM)$^{-1}$ per heme |
|---|---|---|---|---|
| | nm | | nm | |
| Cc3* | 410 | 104 | 530 | 9 |
| Myoglobin‡ | 416 | 121 | 535 | |
| Cytochrome $b_5$§ | 413 | 117 | 523 | |

| MCD | Soret band $\lambda$ | Soret band $\Delta\epsilon$/H (M cm T)$^{-1}$ per heme | Visible band $\lambda$ | Visible band $\Delta\epsilon$/H (M cm T)$^{-1}$ per heme |
|---|---|---|---|---|
| | nm | | nm | |
| Cc3 | 401 | 63 | 552 | 4 |
| | 410 | 0 | 564 | 0 |
| | 417 | −66 | 574 | −9 |
| Myoglobin‡ | 408 | 51 | 555 | 6 |
| | 415 | 0 | 564 | 0 |
| | 423 | −63 | 574 | −10 |
| Cytochrome $b_5$¶ | 406 | 68 | 553 | 9 |
| | 413 | 0 | 562 | 0 |
| | 419 | −88 | 570 | −14 |

*This work.
‡Vickery, Nozawa, and Sauer (1976).
§Ozols and Strittmatter (1964).
¶Vickery, Salmon, and Sauer (1975).

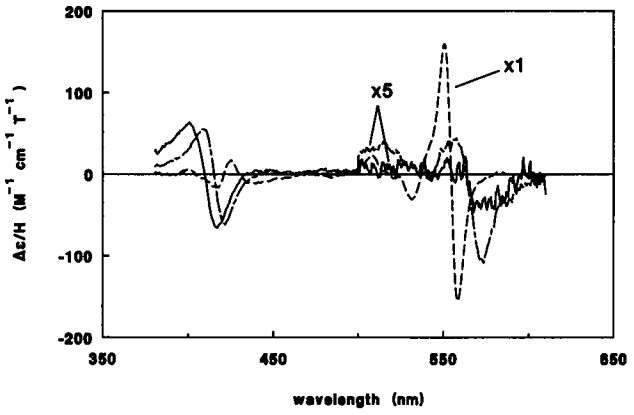


FIGURE 2 Soret and visible band MCD spectra of ferric (——), ferrous (- - - -), and ferrous-CO (— - —) forms of cytochrome $c_3$. The visible bands of ferric and ferrous-CO forms are shown multiplied by a factor of 5.

spin character. For example, the Soret MCD intensities of cytochrome $b_5$ (Table 1) and cyanide-ligated metmyoglobin, in which 100% of the hemes are low spin, are nearly equal and both are greater than the Soret MCD intensity of bis-imidazole axially ligated metmyoglobin (Table 1), which is ~90% low spin. However, the Soret MCD intensity of ferric Cc3, which is 100% low spin, is intermediate between that of cytochrome $b_5$ and bis-histidine metmyoglobin. This apparent discrepancy between spin state and MCD intensity is resolved when account is taken of the weaker extinction coefficient of ferric Cc3 relative to the other two ferric heme proteins.

The visible band MCD of ferric Cc3 is also shown in Fig. 2 and spectral features are detailed in Table 1. The Cc3 spectrum closely resembles the cytochrome $b_5$ spectrum (Dolinger et al., 1974; Vickery et al., 1975) (Table 1) and other bis-histidine heme proteins (Vickery et al., 1976a). The spectral feature corresponding to the $Q_0$ band (zero crossing at 564 nm) has been assigned to Faraday $A$ and $C$ terms in low-spin ferric heme proteins (Vickery et al., 1976a). The weak spectral features in the region between the Soret and $Q_v$ bands (450–520 nm) have been ascribed to charge transfer transitions between the porphyrin and the metal and are thus sensitive to the axial ligation of the iron (Vickery et al., 1976b). In particular, bis-histidine heme proteins, including Cc3, exhibit uniquely characteristic features in this region (Vickery et al., 1976a).

## Ferrous (bis histidine) cytochrome $c_3$

The absorption spectrum of ferrous Cc3 axially ligated to histidines is shown in Fig. 1. The spectral features tabulated in Table 2 agree with published spectra (Meyer and Kamen, 1982). The peak of the broad Soret band ($\lambda_{max}$ 419 nm) is of greater intensity and red-shifted from that of ferric Cc3 (Fig. 1). The Soret bandwidth of ferrous Cc3 is narrower than that of oxidized Cc3, so the Soret transition oscillator strengths are comparable for the two oxidation states. The weaker but well resolved $\alpha$ and $\beta$ bands near 552 and 525

**TABLE 2 Spectral features of the electronic absorption and magnetic circular dichroism of ferrous, bis-histidine, heme proteins**

| Absorption | Soret band $\lambda_{max}$ | Soret band $\epsilon$ (cm mM)$^{-1}$ per heme | Visible band $\lambda_{max}$ | Visible band $\epsilon$ (cm mM)$^{-1}$ per heme |
|---|---|---|---|---|
| | nm | | nm | |
| Cc3* | 419 | 184 | 525 | 16 |
| | | | 552 | 29 |
| Cytochrome $b_5$‡ | 423 | 171 | 526 | 13 |
| | | | 556 | 26 |

| MCD | Soret band $\lambda$ | Soret band $\Delta\epsilon$/H (M cm T)$^{-1}$ per heme | Visible band $\lambda$ | Visible band $\Delta\epsilon$/H (M cm T)$^{-1}$ per heme |
|---|---|---|---|---|
| | nm | | nm | |
| Cc3* | 399 | 5 | 508 | 23 |
| | 417 | −16 | 518 | 0 |
| | 420 | 0 | 531 | −31 |
| | 425 | 17 | 550 | 159 |
| | 430 | 0 | 553 | 0 |
| | 439 | −12 | 558 | −155 |
| Cytochrome $b_5$§ | 415 | −9 | 511 | 25 |
| | 420 | 0 | 522 | 0 |
| | 426 | 20 | 535 | −25 |
| | 432 | 0 | 553 | 185 |
| | 438 | −6 | 557 | 0 |
| | | | 561 | −185 |

*This work.
‡Ozols and Strittmatter (1964).
§Vickery, Salmon, and Sauer (1975).

nm, respectively, are typical of low-spin ferrous heme proteins, e.g., cytochrome $b_5$ (Table 2) and cytochrome *c* (Moore and Pettigrew, 1987).

Fig. 2 shows the MCD spectrum of ferrous Cc3. The extrema and zero crossings are listed in Table 2. The MCD spectra of ferrous Cc3 and another bis-histidine heme protein, cytochrome $b_5$, are strikingly similar (Dolinger et al., 1974; Vickery et al., 1975; Svastits and Dawson, 1986) (Table 2). In the visible region, the relatively intense sigmoidal band with zero crossing at 553 nm and weaker sigmoidal band with zero crossing at 518 nm are associated with the $\alpha$ and $\beta$ band absorptions, respectively. These derivative shaped MCD bands, seen in the spectra of low spin ($S = 0$) ferrous heme proteins such as cytochromes *c* (Vickery et al., 1976a) and $b_5$ (Table 2), are attributed to *A* terms resulting from the degenerate porphyrin electronic excited states. The MCD of the vibrational $\beta$ band is relatively weak due to overlapping *A* terms.

The Soret band MCD of ferrous Cc3 is relatively weak and complex, bearing little resemblance to the derivative of the absorption spectrum that is expected for a Faraday *A* term. Reduction of ferric Cc3 to the ferrous form results in a loss of the relatively intense *C* terms associated with the paramagnetic iron. The spectrum of ferrous Cc3 is very similar to that of ferrous cytochrome $b_5$. By analogy to the latter, we can attribute the complexity of the Soret MCD spectrum of ferrous Cc3 to the presence of a Faraday *B* term overlapping the expected *A* term (Vickery et al., 1976a). The weak positive lobe on the blue edge of the Soret MCD corresponds spectrally to the weak vibronic shoulder of the Soret absorption (Fig. 1).

**TABLE 3 Spectral features of the electronic absorption and magnetic circular dichroism of ferrous, heme proteins axially ligated to CO and histidine**

| | Soret band | | Visible band | |
|---|---|---|---|---|
| Absorption | $\lambda_{max}$ | $\epsilon$ (cm mM)$^{-1}$ per heme | $\lambda_{max}$ | $\epsilon$ (cm mM)$^{-1}$ per heme |
| | nm | | nm | |
| Cc3* | 415 | 149 | 539 | 12 |
| | | | 561 | 11 |
| Myoglobin‡ | 423 | 187 | 542 | 14 |
| | | | 579 | 12 |
| IDO§ | 420 | 210 | 540 | 18 |
| | | | 571 | 21 |
| | Soret band | | Visible band | |
| MCD | $\lambda$ | $\Delta\epsilon$/H (M cm T)$^{-1}$ per heme | $\lambda$ | $\Delta\epsilon$/H (M cm T)$^{-1}$ per heme |
| | nm | | nm | |
| Cc3* | 409 | 55 | 515 | 8 |
| | 415 | 0 | 557 | 9 |
| | 421 | −62 | 563 | 0 |
| | | | 572 | −22 |
| Myoglobin¶ | 417 | 58 | 524 | 12 |
| | 422 | 0 | 565 | 25 |
| | 427 | −62 | 572 | 0 |
| | | | 581 | −40 |
| IDO§ | 415 | 85 | 521 | 10 |
| | 419 | 0 | 560 | 35 |
| | 424 | −90 | 567 | 0 |
| | | | 574 | −50 |

* This work.
‡ Antonini and Brunori (1971).
§ Uchida et al. (1983).
¶ Vickery, Nozawa, and Sauer (1976).

## CO-ligated cytochrome $c_3$

The absorption spectrum of ferrous Cc3-CO is shown in Fig. 1 and the prominent spectral features listed in Table 3. The $\alpha$ and $\beta$ bands are red-shifted, less resolved, of weaker intensity, and of greater bandwidth than the bands in bis-histidine ferrous Cc3 spectrum (Fig. 1). The Cc3-CO absorptions are similar to the ferrous, low-spin forms of myoglobin (Antonini and Brunori, 1971) and indoleamine 2,3-dioxygenase (IDO) (Uchida et al. 1983a) axially ligated to histidine and CO (Table 3). All exhibit poorly resolved $\alpha$, $\beta$ bands relative to bis-imidazole ligated ferrous Cc3 (Fig. 1). The $\beta$ band maximum intensity is greater than the $\alpha$ band maximum intensity for myoglobin and Cc3.

The MCD spectrum of Cc3-CO (Fig. 2 and Table 3) resembles that of low-spin ferrous heme proteins with CO and histidine as axial ligands such as IDO (Uchida et al. 1983a), myoglobin (Vickery et al., 1976b), and horseradish peroxidase (Nozawa et al., 1976). In the Soret band, the symmetric derivative shape and correspondence of the zero crossover with the electronic absorption maximum are consistent with an *A* term arising from degenerate electronic excited states. Both the maximum extinction coefficient and MCD intensity of IDO are greater than the corresponding values of Cc3 as expected for species of comparable bandwidths. (Recall that the intensity of MCD *A* terms scales as the inverse square of the bandwidth (Dawson and Dooley, 1989)).

In the visible, the MCD of Cc3-CO closely resembles that of carbon monoxymyoglobin (Table 3). By analogy to carbon monoxymyoglobin, the asymmetric sigmoidal band (563-nm zero crossing) can be attributed to a Faraday *A* term corresponding to the $\alpha$ absorption transition. The weak feature with a positive extremum near 515 nm can be attributed to an *A* term arising from the $\beta$ transition. The significant overlap of the broad *A* terms of the $\alpha$ and $\beta$ bands results in asymmetry. As predicted by MCD principles, the relatively weak *A* terms of Cc3-CO and carbonmonoxymyoglobin MCD are associated with broad absorption bandwidths, whereas the more intense *A* terms of bis-histidine ferrous Cc3 are associated with narrow absorption bandwidths.

## TRMCD and TROD of CO photolysis

The TROD spectra measured at several delay times after photodissociation of Cc3-CO are shown in Fig. 3 *a*. (The TROD spectrum represents the absorption difference between the transient species and Cc3-CO multiplied by the photolysis yield.) The maximum photolysis yield was obtained with an actinic pulse energy of approximately 30 mJ.

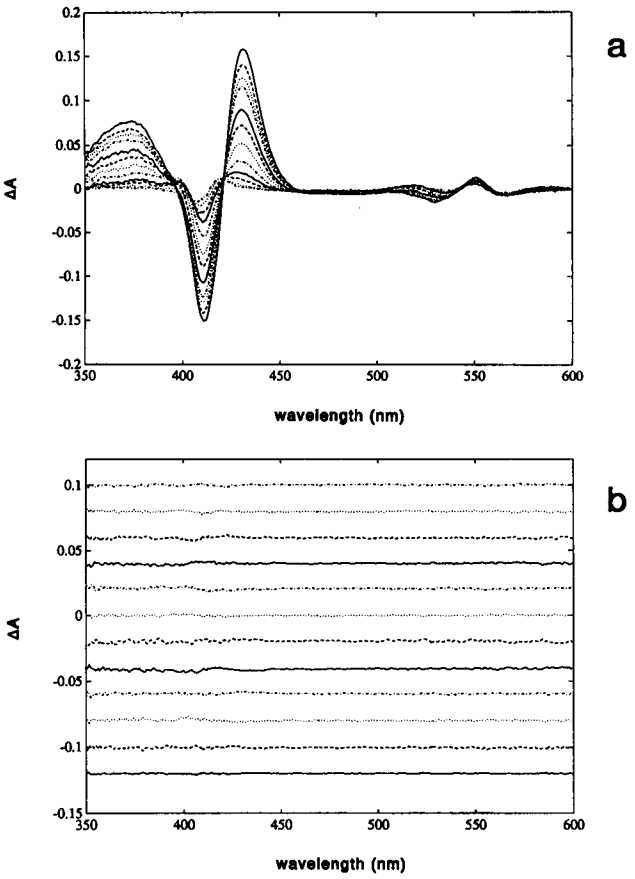


FIGURE 3 (*a*) Time-resolved absorption spectra of Cc3-CO recombination obtained at the following delays after photolysis: 10 ns, 4 μs, 10 μs, 20 μs, 50 μs, 100 μs, 200 μs, 500 μs, 1 ms, 2 ms, 5 ms, and 10 ms. (*b*) Residuals of global kinetic fit to recombination data using four exponentials, lifetimes = 5.7 μs, 62 μs, 425 μs, and 2.9 ms. (The residuals for the different time delays in *a* are offset with the shortest times at the top of graph.)

The peak-to-trough amplitude of the transient spectrum decreased linearly with decreasing photolysis pulse energy for pulse energies below 30 mJ and the profile of the transient spectrum was independent of pulse energy. The bleach centered near 414 nm and the positive absorbance centered near 434 nm both decay monotonically with time. The spectral bandshape of the transient spectra are indistinguishable with time until ~1 ms and longer delays. The spectra at the long delays show a blue shift of both the minima (bleach) and maxima extrema in the Soret band. These long-time spectra are quite similar to the difference spectrum between ground state ferrous (bis-histidine) Cc3 and Cc3-CO (Fig. 4 *a*). Finally, there is a very slow CO recombination process over a timescale greater than 1 second. (Incomplete recombination required a continual flow of fresh sample in order to signal average TROD measurements obtained at various time delays at the 1–2 Hz data collection rate.) The time scale of this slow recombination is consistent with the thermal dissociation of the sixth coordinate histidine and subsequent second order recombination of free CO with the iron. A global fitting analysis (Goldbeck and Kliger, 1993) of the TROD spectra obtained at all time delays yielded 4 first order kinetic time constants of 5.7 μs, 62 μs, 425 μs, and 2.9 ms (the fifth, >1 s, process was too slow and small in amplitude for a reliable quantitative fit). The residuals of the global analysis are plotted in Fig. 3 *b*. Analysis of TROD data obtained with a much smaller actinic pulse (3 mJ rather than 30 mJ) yielded the same time constants within experimental error.

In principle, the spectra of physical intermediates and their rates of formation and decay for a kinetic mechanism involving only first order processes can be related to the observed rate constants and associated basis spectra by matrix diagonalization methods (Millhauser and Oswald, 1988). In the simplest model, in which each exponential decay process proceeds in parallel (A → B; A → C; A → D; and A →E), the microscopic rate constants and intermediate spectra are simply equal to the observed constants and their basis spectra. However, in more complex models the number of microscopic rate constants can exceed the number of observed rate constants and additional information (e.g., equilibrium constants, back reaction rate constants) is then needed to complete the analysis. The recombination kinetics after photolysis of Cc3-CO are sufficiently complex that global fitting

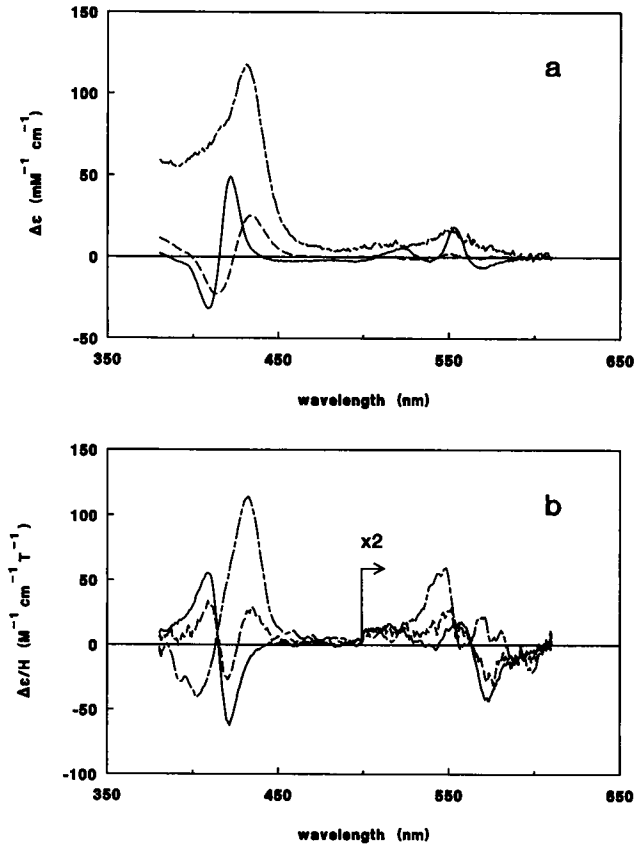


FIGURE 4 (*a*) Absorption difference spectra of (ferrous) bis-histidine Cc3 minus Cc3-CO (——) and photolyzed Cc3-CO minus Cc3-CO (- - - -), and the calculated absolute spectrum of photolyzed Cc3-CO (— - —) (see text). (*b*) MCD spectra of Cc3-CO (——), mixture of (~30%) photolyzed and (~70%) unphotolyzed Cc3-CO sampled over the time interval 0–4 μs after photolysis (- - - - -), and calculated TRMCD spectrum (0–4 μs) of photolyzed Cc3-CO (— - —). The visible band region is shown expanded by a factor of 2.

methods could not be used to obtain unique spectra and rate constants for physical intermediates from the present data. Consistent with this complexity, attempts at applying a simple parallel model and a simple sequential (A → B → C → D → E) model did not yield realistic (i.e., nonnegative) absolute absorption spectra for intermediates. An outline of a kinetic scheme for CO recombination in Cc3 is discussed further below.

Fig. 4 *a* shows the TROD spectrum averaged over 2.7 μs immediately after laser photolysis of Cc3-CO. The prominent features are a broad bleach ($\lambda_{min}$ 414 nm) and a broad positive lobe ($\lambda_{max}$ 434 nm) in the Soret and very weak structural features in the visible region associated with the Q bands. The absorption difference spectrum between ground state ferrous Cc3 and ground state Cc3-CO is also shown in Fig. 4 *a*. The red shift of the TROD spectrum relative to the ground state difference spectrum indicates that the Soret absorption of the transient species is red-shifted from the ferrous, bis-histidine Cc3 absorption.

Determination of the absolute absorption spectrum of the transient species requires knowledge of the photolysis yield for Cc3-CO, which cannot be accurately determined from the present data. Nevertheless, a lower bound can be estimated for the photolysis yield by adding the ground state Cc3-CO spectrum, scaled by a multiplicative factor, to the TROD spectrum. Using the criteria that the resulting spectrum, the absorption spectrum of the transient species, should be everywhere positive and have a single broad band in the Soret, we estimate the photolysis yield at saturation to be ~30%. If this is further taken as an estimate for the photolysis *quantum* yield, it implies a geminate recombination quantum yield as large as 70%. However, the actual photolysis quantum yield can be lower than the observed yield due to secondary absorption of a photon when geminate recombination and other, nondissociative relaxation processes are rapid compared to the actinic pulse duration. Since the four hemes are spectrally indistinct, it was not possible to obtain the microscopic photolysis yield of each heme. The 30% yield is an estimate of the average photolysis for the four hemes. If the hemes are identical, this corresponds to microscopic yields of ~0.3 for each heme. If they are nonidentical, the photolysis yield of a particular heme may be as large as unity, in which case the others would be nearly nil.

The absolute absorption spectrum calculated above for the transient photolysis product is shown in Fig. 4 *a*. The most important spectral features are a broad Soret absorption that is red-shifted from ferrous Cc3 and a broad absorbance in the visible. The spectral features of the Cc3-CO transient are summarized in Table 4, along with the spectral features of five-coordinate, high-spin ferrous heme proteins, viz., IDO (Uchida et al., 1983b) and deoxymyoglobin (Antonini and Brunori, 1971). The Soret absorptions of each of the high-spin ferrous proteins as well as the Cc3-CO transient are red-shifted and of weaker peak intensity than the corresponding CO-ligated proteins (Table 3). Also, the visible band absorptions consist of a single band whose absorption maximum lies between the α and β transitions seen in the corresponding CO-ligated form (Table 3). These similarities suggest that the transient species immediately subsequent to laser photolysis of Cc3-CO is a high-spin, five-coordinate heme protein. (The close similarity of the spectrum calculated for the Cc3 transient and authentic pentacoordinate hemeproteins also supports the validity of the photolysis yield estimate used in the calculation.)

**TABLE 4 Spectral features of the electronic absorption and magnetic circular dichroism of ferrous, five-coordinate, high-spin heme proteins**

| | Soret band | | Visible band | |
|---|---|---|---|---|
| Absorption | $\lambda_{max}$ | ε (cm mM)$^{-1}$ per heme | $\lambda_{max}$ | ε (cm mM)$^{-1}$ per heme |
| | nm | | nm | |
| Cc3 transient* | 431 | 117 | 548 | 17 |
| Myoglobin‡ | 434 | 115 | 556 | 12 |
| IDO§ | 429 | 100 | 559 | 18 |

| | Soret band | | Visible band | |
|---|---|---|---|---|
| MCD | λ | Δε/H (M cm T)$^{-1}$ per heme | λ | Δε/H (M cm T)$^{-1}$ per heme |
| | nm | | nm | |
| Cc3 transient* | 400 | −46 | | |
| | 415 | 0 | | |
| | 432 | 121 | | |
| Myoglobin¶ | 420 | −32 | 548 | 6 |
| | 427 | 0 | 579 | 0 |
| | 437 | 120 | 594 | −8 |
| IDO‖ | 415 | −25 | 528 | 8 |
| | 425 | 0 | 550 | 9 |
| | 435 | 110 | 572 | 0 |
| | | | 589 | −9 |

* This work.
‡ Antonini and Brunori (1971).
§ Uchida et al. (1983).
¶ Vickery, Nozawa, and Sauer (1976).
‖ Dawson and Dooley (1989).

The TRMCD spectrum recorded after laser photolysis (0–4 μs) of Cc3-CO is shown in Fig. 4 *b*. This spectrum is a composite of the MCD of the unphotolyzed Cc3-CO and the transient species. Photolysis decreases the Cc3-CO concentration, resulting in a marked decrease of the *A* term intensities at 409 and 421 nm. Additionally, a relatively strong positive lobe ($\lambda_{max}$ 434 nm) appears in the transient spectrum. In the visible, the differences between ground state Cc3-CO and the TRMCD spectra are less dramatic. A modest decrease of the intensity of the negative lobe of the Cc3-CO spectrum ($\lambda_{min}$ 572 nm) is evident in the TRMCD spectrum.

The relationship of the TRMCD spectrum after incomplete photolysis of Cc3-CO to the MCD spectra of Cc3-CO and the (promptly formed) photolysis transient can be expressed as

$$\mathrm{TRMCD} = (1 - \theta) \cdot \mathrm{MCD_{CO}} + \theta \cdot \mathrm{MCD_{tr}}$$

where $\mathrm{MCD_{CO}}$ and $\mathrm{MCD_{tr}}$ are the MCD spectra of Cc3-CO and the transient species, respectively, and θ is the fraction of sample photolyzed. The spectrum of the transient species can be obtained by subtracting the Cc3-CO MCD spectrum,

scaled to account for the photolysis yield, from the TRMCD spectrum. An estimate of the MCD spectrum of the transient species, calculated with the $\theta$ value obtained from the TROD data, is shown in Fig. 4 *b*. The MCD spectral features of the transient species are similar in the Soret region to those of five-coordinate, high-spin ($S$ = 5/2) ferrous myoglobin (Vickery et al., 1976b) and IDO (Dawson and Dooley, 1989), as shown in Table 4. The MCD spectra of all three species exhibit an asymmetric Soret band with negative blue lobe and stronger positive red lobe. The Soret MCD spectrum of each of the high spin heme proteins is red-shifted from the corresponding ferrous, CO-ligated spectrum (Table 3). The deoxymyoglobin spectrum has been ascribed to Faraday $C$ terms arising from the spin-orbit coupling of the degenerate iron spin states ($S$ = 2) with the porphyrin $\pi$-$\pi^*$ transitions (Vickery et al., 1976b). By analogy to deoxymyoglobin, we thus attribute the Soret MCD of the Cc3-CO transient formed immediately after laser photolysis to $C$ terms of five-coordinate, high-spin ($S$ = 2), ferrous Cc3.

Further evidence for complexity in the recombination of CO with the protein can be seen in the TRMCD spectra of Fig. 5. Of particular interest is the temporal evolution of the TRMCD spectra in the visible region. Immediately after photolysis, the TRMCD spectrum consists of broad and relatively weak bands. By 1.2 ms after photolysis, a clear sigmoidal band centered near 550 nm has appeared. This spectrum is consistent with the fact that bis-histidine ferrous Cc3 exhibits a sharp, relatively intense band in this region (Fig. 2). The TROD spectra at times greater than 1 ms also indicate the presence of bis-histidine ferrous Cc3. Interestingly, the appearance of this bis-histidine Cc3 band can be seen in the TRMCD spectra at times as early as 50 $\mu$s (Fig. 5), although the presence of the low spin Cc3 is not as clearly evident in the TROD spectra at such early times. The weakness of the Q-band MCD of Cc3-CO and five-coordinate high-spin hemes relative to the intense $A$-term bands exhibited by ferrous bis-histidine Cc3 accounts for the high sensitivity of MCD to the latter species. The rapid binding of histidine in Cc3, shown here by TRMCD spectroscopy, has

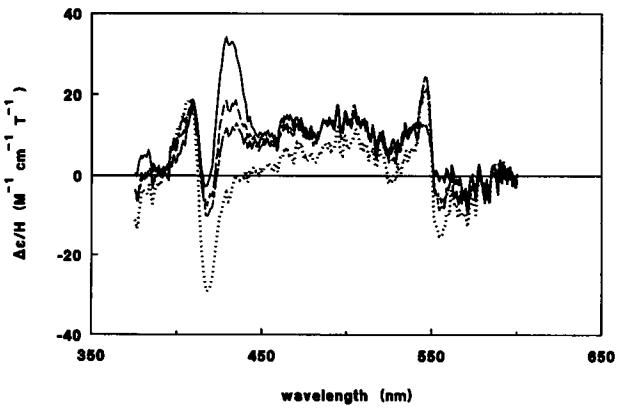


FIGURE 5 TRMCD spectra of Cc3-CO recombination after photolysis (4-$\mu$s sampling gate): 0 $\mu$s (——), 50 $\mu$s (- - - -), 400 $\mu$s (— - —), and 1.2 ms (·····).

a precedent in the photolysis reactions of 1-methylimidazole-heme-CO complex studied by Traylor et al. (1992). The second-order rate constant for binding of imidazole solvent to the photodissociated complex was observed in that study to be $2 \times 10^8$ $M^{-1}$ $s^{-1}$, comparable to CO binding rate constants. Further support for fast histidinyl recombination in Cc3 comes from the observation that recombination of histidine photodissociated from bis-histidine axially ligated hemeproteins can proceed in picoseconds (Jongeward et al., 1988).

The maximum photolysis yield of Cc3-CO is low compared to other hemeproteins that bind CO. One mechanism that may account for the lower photolysis yield of free CO is geminate recombination. Although our nanosecond spectra show no evidence of geminate CO recombination on the 5–500-ns time scale (data not shown), this does not rule out recombination of photodissociated CO within the nanosecond laser pulse width. Geminate recombination is believed to be enhanced by a "closed" distal heme pocket (Hobbs et al., 1990). Because of the large solvent exposure of the hemes in bis-histidine Cc3 (Higuchi et al., 1984), it would be surprising if geminate recombination is the predominant relaxation mechanism, although the structure of the CO complex is not known. In this regard, it is possible that the tertiary structure of the CO-ligated Cc3 may not be as open, thus restricting CO migration from the heme pocket. In particular, the distal histidine, which occupies the sixth axial site on heme in the absence of CO, may be positioned within the pocket by the conformation of the protein in a way that hinders CO diffusion out of the pocket. (Solving the x-ray structure for a Cc3-ligand complex could test this hypothesis, as could TRCD spectroscopy of the protein amide and histidine bands after photolysis.) TROD experiments with 30-ps time resolution show that if geminate recombination does occur, it must be largely complete in less than 30 ps (D. B. O'Connor, unpublished results). Because recombination of a geminate heme · · · CO contact pair typically requires nanoseconds in hemeproteins and imidazole-heme complexes (Traylor et al., 1992), it seems more likely that any ultrafast relaxation goes mainly through nondissociative decay channels of electronically excited Cc3-CO. As noted by Chance et al. (1990), it seems reasonable to expect that the branching of photoexcited hemeprotein-ligand complexes between dissociative and nondissociative channels is influenced by the proximal heme pocket configuration. In the case of Cc3, it further seems reasonable that an unusually intrusive configuration of histidine in the distal pocket could perturb electronic decay rates and account for the unusual branching ratio.

The possibility of multiheme photolysis within Cc3 raises the question of heme-heme interaction and its possible influence on CO photolysis and recombination. The proximity of the four hemes to one another, with iron-iron distances of 11.0–17.8 Å (Higuchi et al., 1984), suggests that heme interactions could affect their ligand binding properties. If more than one heme per protein is dissociated at higher pulse energies and the recombination is cooperative (i.e., the rate

of recombination to a particular heme depends on the degree of ligation of the other hemes) then the recombination kinetics will depend on actinic pulse energy. Multiheme photolysis is indeed a strong likelihood for the photolysis conditions used in the present study. Simple probability theory shows that if the probability of photolysis at a particular heme is 0.3, then 45% of the hemes photolyzed in a tetraheme protein (with identical, noninteracting hemes) will have photolyzed neighbors. This percentage drops to 23% when the heme photolysis yield is halved. That the recombination kinetics are, within experimental error, independent of pulse energy suggests that either one heme per protein dissociates or that CO recombination is noncooperative.

## Microscopic kinetics of CO recombination

We briefly consider the simplest elements necessary to a kinetic scheme describing the recombination reactions of CO with Cc3, recognizing that a definitive picture of this kinetically complex system must remain a goal for future studies. If the kinetics at each heme are independent of heme-heme interactions, then we can write a generic scheme, such as the one shown below, that applies separately for each site. Photolysis of the CO-complex 1 creates a five-coordinate species 2 (for simplicity, ultrafast processes such as geminate recombination are left implicit in the photoexcitation step). Species 2 either recombines with free CO to reform 1, with a second-order rate constant, $k_{21}$, or forms the bis-histidine intermediate 3 with a first-order rate constant, $k_{23}$. Thermal dissociation of the CO-complexed and bis-histidine species are described by the first-order rate constants $k_{12}$ and $k_{32}$, respectively. With four rate constants for each heme, a total of 16 microscopic rates determines the overall kinetics. However, the spectral similarity of the hemes may not allow differing rate constants for individual hemes to be distinguished. Furthermore, some rate constants may not be kinetically important. The high stability of the CO complex, for example, prevents significant thermal dissociation of complex during the photolysis reactions (we measured $k_{12} = 4 \cdot 10^{-3}$ s$^{-1}$ from the time evolution of absorbance at 422 nm after injection of a 6-$\mu$l volume of approximately 1 mM Cc3-CO solution into a 3-ml volume of degassed dithionite buffer). The branching ratio of 1 to 3 is determined by $k_{21}[\mathrm{CO}]/k_{23}$. Fig. 5 shows that roughly comparable amounts of 3 and 1 are formed after photolysis. This is consistent with the presence of a branching ratio on the order of unity at a particular heme or with the simultaneous presence of hemes that branch oppositely to favor production of 3 or 1. In either case, the implication that $k_{23}$ can be comparable to $k_{21}[\mathrm{CO}]$ is consistent with the observation mentioned above that the rate constant of second-order binding of imidazolic ligands to imidazole-heme model compound is comparable with CO binding rate constants. A $k_{21}$ value on the order of $10^8$ M$^{-1}$ s$^{-1}$ is typical for CO recombination in hemeproteins, corresponding to a pseudo first-order rate constant of $10^5$ s$^{-1}$ at 1 atm CO. The fastest rate constant observed in Cc3 is in good agreement with this value. However, in the proposed scheme the fastest rate observed for each heme corresponds to $k_{21}[\mathrm{CO}] + k_{23}$ and knowledge of the branching ratio is necessary to determine the microscopic rate constants. The next three observed rate constants are each successively slower by an order of magnitude. These may correspond to $k_{21}$ values in hemes where CO recombination is sterically hindered, perhaps by a distal histidine positioned by the conformation of the protein so as to block the sixth axial site, or to corresponding variations in $k_{23}$. The slowest rate constant observed in Cc3 is separated by three orders of magnitude from the others and probably corresponds to $k_{32}$, thermal dissociation of bis-histidine Cc3. (We performed Cc3 + CO mixing reactions [data not shown] that showed that $k_{32}$ can be as small as $2.5 \cdot 10^{-2}$ for at least some of the four hemes in the equilibrium bis-histidinyl coordinated enzyme. It is possible, however, that histidine dissociation from the bis-histidine photolysis product may be faster. The structure of the heme pocket may differ between flash-photolyzed Cc3 and the thermally dissociated five-coordinate heme, leading to the possibility of different histidine recombination and dissociation rates for the two species.) The overall picture then is that photodissociation of 1 produces 2 within picoseconds, which branches to reform 1 or form the second transient intermediate, 3. The prompt return of 2 to 1, perhaps represented by different $k_{21}$ values for the different hemes, proceeds on a timescale from microseconds to milliseconds. Finally, the slow dissociation of 3 to 2 and its complete return to 1 requires seconds.

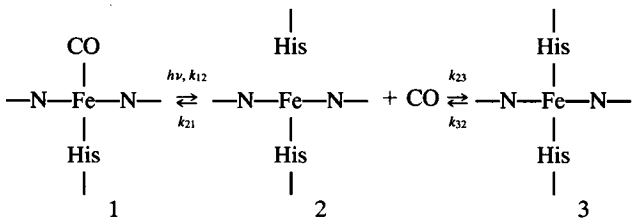


## CONCLUSIONS

The UV-visible absorption and MCD spectral properties of equilibrium ferric, ferrous, and CO-ligated forms of Cc3 are largely determined by the oxidation, spin, and axial coordination state of the heme centers. The spectra of ferric and ferrous Cc3 are thus characteristic of bis-histidine axially coordinated hemeproteins, such as cytochrome $b_5$, while the absorption and MCD spectra of the Cc3-CO complex resemble those of the histidine-CO-ligated hemeprotein myoglobin-CO. As in hemoglobin, the recombination kinetics after photodissociation of CO from this tetraheme protein are complex, apparently involving at least five rate processes, although evidence for cooperativity in heme-CO binding was not found in Cc3. Time-resolved absorption and MCD spectroscopy of the initial photolysis intermediate show the presence of a pentacoordinate, high-spin heme species. Subsequently, the distal histidine competes with CO for rebinding to the axial heme sites left vacant by CO photodissociation, contributing to at least some of the complexity observed in the recombination kinetics. This competition between ex-

ogenous and endogenous ligand rebinding is most clearly revealed by the visible band TRMCD signal of the bis-histidine intermediate, which is found to be well developed by 50 $\mu$s after photolysis. The recovery of equilibrium heme-CO binding in Cc3 is unusually slow for a hemeprotein, probably due in part to the additional kinetic barrier encountered by CO in replacing histidine in the bis-histidine intermediate. A similar mechanism, transient coordination of an endogenous ligand to the sixth axial site of the heme, also appears to interfere with CO recombination in another, dissimilar hemeprotein, cytochrome *c* oxidase (Woodruff et al., 1991; Goldbeck et al., 1991). Thus, the study of CO photodissociation and rebinding in Cc3, a protein in which the binding of exogenous ligands is apparently unrelated to physiological function, may help in understanding the interaction of mitochondrial oxidase with ligands such as CO and its physiological oxidant, $O_2$.

Financial support for this work was provided by grants from the National Institutes of Health (GM-38549) (to D. S. Kliger) and the Office of Naval Research (to M. A. Cusanovich).

## REFERENCES


Akutsu, H., J. H. Hazzard, R. G. Bartsch, and M. A. Cusanovich. 1992. Reduction kinetics of the four hemes of cytochrome $c_3$ from *Desulfovibrio vulgaris* by flash photolysis. *Biochim. Biophys. Acta.* 1140:144–156.

Antonini, E., and M. Brunori. 1971. Hemoglobin and Myoglobin in Their Reaction with Ligands. North Holland, Amsterdam. pp. 17–19.

Chance, M. R., S. H. Courtney, M. D. Chavez, M. R. Ondrias, and J. M. Friedman. 1990. $O_2$ and CO reactions with heme proteins: quantum yields and geminate recombination on picosecond time scales. *Biochemistry.* 29:5537–5545.

Dawson, J. H., and D. M. Dooley. 1989. Magnetic circular dichroism spectroscopy of iron porphyrins and heme proteins. *In* Iron Porphyrins Part III. A. B. P. Lever and H. B. Gray, editors. VCH, New York. pp. 1–136.

Dolinger, P. M., M. Kielczewshi, J. R. Trudell, G. Barth, R. E. Linder, E. Bunnenberg, and C. Djerassi. 1974. Magnetic circular dichroism studies XXV. A preliminary investigation of microsomal cytochromes. *Proc. Nat. Acad. Sci. USA.* 71:399–403.

Drucher, H., L. L. Campbell, and R. W. Woody. 1970. Optical rotatory properties of the cytochromes $c_3$ from three species of *Desulfovibrio. Biochemistry.* 9:1519–1527.

Goldbeck, R. A., T. D. Dawes, S. J. Milder, J. W. Lewis, and D. S. Kliger. 1989. Measurement of magnetic circular dichroism (MCD) on a nanosecond timescale. *Chem. Phys. Lett.* 156:545–549.

Goldbeck, R. A., T. D. Dawes, Ó. Einarsdóttir, W. H. Woodruff, and D. S. Kliger. 1991. Time-resolved magnetic circular dichroism spectroscopy of photolyzed carbonmonoxy cytochrome *c* oxidase (cytochrome $aa_3$). *Biophys. J.* 60:125–134.

Goldbeck, R. A., and D. S. Kliger. 1993. Nanosecond time-resolved absorption and polarization dichroism spectroscopies. *Meth. Enzymol.* 226: 147–177.

Higuchi, Y., M. Kusonoki, Y. Mastuura, N. Tasouka, and M. Kakudo 1984. Refined structure of cytochrome $c_3$. *J. Mol. Biol.* 172:109–139.

Hobbs, J. D., R. W. Larsen, T. E. Meyer, J. H. Hazzard, M. A. Cusanovich, and M. R. Ondrias. 1990. Resonance Raman characterization of *Chromatium vinosum* cytochrome *c'*. Effect of pH and comparison of equilibrium and photolyzed carbon monoxide species. *Biochemistry.* 29:4166–4174.

Ishimoto, M., J. Koyama, and Y. Nagai. 1954. A cytochrome and a green pigment of sulfate-reducing bacteria. *Bull. Chem. Soc. Jpn.* 27:564–565.

Jongeward, K. A., D. Magde, D. J. Taube, and T. G. Traylor. 1988. Picosecond kinetics of cytochromes $b_5$ and *c*. *J. Biol. Chem.* 263:6027–6030.

Kimura, K., Y. Nakahara, T. Yagi, and H. Inokuchi. 1979. Electrical conduction of hemoprotein in the solid phase: anhydrous cytochrome $c_3$ film. *J. Chem. Phys.* 70:3317–3323.

Lewis, J. W., and D. S. Kliger. 1987. Recent advances in time-resolved circular dichroism spectroscopy. *Rev. Chem. Interm.* 8:367–398.

Meyer, T. E., and M. D. Kamen. 1982. New perspectives on c-type cytochromes. *Adv. Protein Chem.* 35:105–212.

Millhauser, G. L, and R. E. Oswald. 1988. A reevaluation of the mathematical models for simulating single-channel and whole-cell ionic currents. *Synapse (NY).* 2:97–103.

Moore, G. R., and G. W. Pettigrew. 1987. Cytochromes *c*: Biological Aspects. Springer Verlag, Berlin.

Moore, G. R., and G. W. Pettigrew. 1990. Cytochromes *c*: Evolutionary, Structural and Physiochemical Aspects. Springer Verlag, Berlin.

Nakahara, Y., K. Kimura, H. Inokuchi, and T. Yagi. 1980. Electrical conductivity of an anhydrous cytochrome $c_3$ film as a function of temperature and ambient pressure. *Chem. Phys. Lett.* 73:31–34.

Niki, K., Y. Kawasaki, Y. Kimura, Y. Higuchi, and N. Yasouka. 1987. Surface-enhanced Raman scattering of cytochromes $c_3$ adsorbed on silver electrodes and their redox behavior. *Langmuir.* 3:982–986.

Nozawa, T., N. Kobayashi, and M. Hatano. 1976. Magnetic circular dichroism studies on horseradish peroxidase. *Biochim. Biophys. Acta.* 427: 652–662.

Ozols, J., and P. Strittmatter. 1964. The interaction of porphyrins and metalloporphyrins with apocytochrome $b_5$. *J. Biol. Chem.* 239:1018–1023.

Postgate, J. R. 1954. Presence of cytochrome in an obligate anaerobe. *Biochem. J.* 56:xi-xii.

Suh, B. J., and J. M. Akagi. 1969. Formation of thiosulfate from sulfite by *Desulfovibrio vulgaris. J. Bacteriol.* 99:210–215.

Svastits, E. W., and J. H. Dawson. 1986. Models for ferrous cytochrome $b_5$: sign inversions in the magnetic circular dichroism spectra of bis-imidazole ferrous porphyrin systems. *Inorg. Chim. Acta.* 123:83–86.

Tamura, A., T. Kawate, M. Ogata, and T. Yagi. 1988. Interaction of cellular hydrogenase, cytochrome $c_3$. *J. Biochem. (Tokyo).* 104:722–726.

Traylor, T. G., D. Magde, D. J. Taube, K. A. Jongeward, D. Bandyopadhyay, J. Luo, and K. N. Walda. 1992. Geminate recombination of carbon monoxide complexes of hemes and heme proteins. *J. Am. Chem. Soc.* 114: 417–429.

Uchida, K., T. Shimizu, R. Makino, K. Sakaguchi, T. Iizuka, Y. Ishimura, T. Nozawa, and M. Hatano. 1983a. Magnetic and natural circular dichroism of L-tryptophan 2,3-dioxygenases and indoleamine 2,3-dioxygenase. I. Spectra of ferric and ferrous high spin forms. *J. Biol. Chem.* 258:2519–2525.

Uchida, K., T. Shimizu, R. Makino, K. Sakaguchi, T. Iizuka, Y. Ishimura, T. Nozawa, and M. Hatano. 1983b. Magnetic and natural circular dichroism of L-tryptophan 2,3-dioxygenases and indoleamine 2,3-dioxygenase. II. Spectra of their ferric cyanide and ferrous carbon monoxide complexes and in oxygenated form. *J. Biol. Chem.* 258:2526–2533.

Vickery, L. E., A. G. Salmon, and K. Sauer. 1975. Magnetic circular dichroism studies on microsomal aryl hydrocarbon hydroxylase: comparison with cytochrome $b_5$ and cytochrome P-$450_{cam}$. *Biochim. Biophys. Acta.* 386:87–98.

Vickery, L. E., T. Nozawa, and K. Sauer. 1976a. Magnetic circular dichroism studies of low spin cytochromes. Temperature dependence and effects of axial coordination on the spectra of cytochrome *c* and cytochrome $b_5$. *J. Am. Chem. Soc.* 98:351–357.

Vickery, L. E., T. Nozawa, and K. Sauer. 1976b. Magnetic circular dichroism studies of myoglobin complexes. Correlations with heme spin state and axial ligation. *J. Am. Chem. Soc.* 98:343–350.

Woodruff, W. H., Ó. Einarsdóttir, R. B. Dyer, K. A. Bagley, G. Palmer, S. J. Atherton, R. A. Goldbeck, T. D. Dawes, and D. S. Kliger. 1991. Nature and functional implications of the cytochrome $a_3$ transients after photodissociation of CO-cytochrome oxidase. *Proc. Natl. Acad. Sci. USA.* 88: 2588–2592.

Yagi, T., and K. Maruyama. 1971. Purification and properties of cytochrome $c_3$ of *Desulfovibrio vulgaris*, Miyazaki. *Biochim. Biophys. Acta.* 243: 214–224.